

Experimental and Numerical Analysis on Failure of Soil Slopes Induced by Increasing Pore Water Pressure

Godfred Amponsah

New Mexico Institute of Mining and Technology,
Socorro, NM

Mehrdad Razavi

New Mexico Institute of Mining and Technology,
Socorro, NM

ABSTRACT

Slope failures very commonly occur during a long period of heavy rainfall and groundwater rise. The failures pose a substantial risk to people, infrastructure, and equipment downslope. In the recent past, the mining industry has faced an increase in tailings dam failure due to several reasons including pore pressure increases in the dams. Many failures have been observed to occur during times of water level fluctuations but the critical factors that influence the initiation of slope failures still need to be adequately clarified. To investigate these factors, laboratory experiments were conducted on model sandy slopes to determine pore pressure-induced slope failure initiation.

This study also presents a method to examine water seepage through soil slopes using an ultraviolet (UV) dye and a UV flashlight. The small-scale model test simulation demonstrated failures induced by either water percolation from the upslope tank at a constant level or by raising the water level at intervals. A bottom chamber fully filled with water to replicate groundwater rise was also simulated. The soil slope was monitored at every stage to study the deformations and behavior until failure occurred.

Results gathered from the controlled laboratory conditions were useful for the verification of the numerical modeling method created in the computer program Slide. The analysis showed that slope failure always occurred when

the toe was fully saturated. High pore pressures and seepage forces reduce the shear force at the toe to almost zero causing it to slide. A comparison of slope height to water level also indicated an average of 96% water level to cause a failure. At this point, the soil slope is fully saturated and has no matric suction. The findings in this study show that, by monitoring the moisture content of slopes, failures can be predicted.

INTRODUCTION

Soil has so many uses in our day-to-day life. Designing structures in soil requires engineering judgments and calculations. Soil particles naturally create friction between grains, and when this bond is broken, there is instability. Evaluating the causes of soil slope failure is essential in civil and mining engineering, and a significant cause of this is an increase in pore-water pressure. From this, it is necessary to perform laboratory tests to understand better how such failures occur. Several techniques are available to induce slope movement and failure, such as rainfall, using a shake table, and increasing pore-water pressure. All these methods require a laboratory set-up, which is time-consuming and requires precision. These tools can prove useful if the monitored slope is visible and not significantly affected by massive external physical contact such as shaking of the monitored slope. Any physical contact with an observed

phenomenon can affect the outcome and, in some situations, alter results.

Generally, in natural slopes, a boundary line divides the unsaturated soil and the saturated soil. Above the line, the pore water pressure of the unsaturated soil is negative to zero, while the water pressure of the saturated soil below the boundary line is positive (Fredlund and Rihardjo, 1993) It was found that the development of pore fluid pressures within soil masses, influenced by both mechanical and physico-chemical effects, affects the magnitude of inter-granular or effective stresses. These inter-granular stresses play a crucial role in controlling the shear and compression behavior of soil in many instances (Mitchell 2013)

The principle of effective stress is one of the most essential concepts of modern soil mechanics. It has been found useful as a basis for the understanding of stress and strain characteristics of soils and has become increasingly important in practical engineering problems. An increase in pore water pressure has caused so many landslides and slope failures in both mining and civil engineering.

In the mining industry, one major cause of tailings dam failure has been pore pressure increase. It was found that gradual rise in saturation levels and pore pressure can initiate static liquefaction and flow sliding failures (Eckersley 1990; Martin and McRoberts 1999). Slope stability is influenced by excess pore water pressure, which can result from factors such as prolonged and heavy rainfall, rising groundwater, or earthquakes. (Chin-C and Chien-Li 2013). Some efforts have also been made to develop a predictive warning system for rainfall-induced slope failures (e.g., Johnson and Sitar 1990; Anderson and Thallapally 1996; Rahardjo 1999; Fannin and Jaakkola 1999). Previous studies have shown that Soil-water characteristic curves (SWCC) and soil permeability functions pertinent to specific soils along with numerical analysis tools, can be used to capture the timing of wetting front propagation and the resulting slope failures (Cai and Ugai, 2004; Kim et al., 2004; Gerscovich et al., 2006; Cho, 2009; Tu et al., 2009; Montrasio et al., 2009; Rahimi et al., 2010).

Spence and Gumar (1997), observed an increase in the pore water pressure in small scale laboratory flow slides using flumes test. They concluded that the pore water pressures are reasonably predicted by using the Coulomb failure criterion and assuming equilibrium of the driving and resisting forces.

A significant disadvantage of many non-contact measurement and experiment is the high cost of materials and tools. Finite element method is a powerful tool that can be used to model such laboratory experiments. Besides, numerical methods such as finite element method can be

used to study the boundary conditions and scenarios which are not easy to implement in the laboratory tests. However, it is necessary to use mathematics to comprehensively understand and quantify any physical aspects such as structural or fluid behavior.

Numerical modeling techniques rely on mathematical algorithms, employing approximations and appropriate assumptions to streamline complex problems. These models further explore the impact of factors such as slope geometry, soil properties, and the dynamics of water level changes. Numerical studies have been generally used to simulate and provide an improved understanding of slope performance and failure mechanisms related to water changes. (Jia et al. 2009).

The use of dye to trace fluid flow is common in the automobile, health, and beauty industry. It helps in detecting traces in its path and is very fundamental when a visible mark is needed. In soil mechanics, it can help with identifying traces of water movement. Seepage forces are generated on the individual soil grains when water flows through soil. These forces, if large enough, can reduce the effective stresses to zero, essentially making the soil a dense liquid called quicksand. Infiltration and Seepage analyses are important tools to assess the susceptibility of seepage failure in dams and to study hydraulic conditions for analyzing the stability of dam slopes (Chen and Zhang, 2006).

In this research, a finite element analytical tool was used to simulate a simple slope failure caused by an increase in pore-water pressure. A laboratory experiment is conducted using the same soil parameters and properties and compared to the results of the analytical tool when there is a failure. Moreover, seepage was studied.

2.1 Objectives

The main objectives of this research are to:

1. Study the flow of water through a sandy soil slope.
2. Detect and monitor seepage of water using an ultraviolet (UV) dye.
3. Induce slope failure by increasing pore-water pressure and monitoring at the laboratory.
4. Create a numerical model using Slide code.

MATERIALS AND METHODS

3.1 Introduction

This chapter explains the materials and experimental methods used. The soil properties are discussed first, and then the process of making the experimental test box. After these, the procedures of the experiments are explained in depth. Finally, filming with the camera for comparison is

also described. Given the initial conditions at the laboratory, a numerical model analysis simulation was performed to compare the results.

3.2 Soil Properties

The soil used in this experiment was a sandy soil obtained from a site near the Energetic Materials Research and Testing Center (EMRTC) at the New Mexico Tech campus, Socorro, NM. To better understand the soil used for the experiments, it is essential to know the engineering properties of the sand. The sandy soil has a fine texture, brown color, and has angular shape grains. The soil is odorless and has no organic material present in it.

To classify the soil, a sieve analysis test was performed according to ASTM-D422 to ascertain the grain size distribution. The particle size distribution was measured, and the result is shown in Figure 1. The soil is classified as poorly graded sand (SP) based on the grain size distribution results.

The internal friction angle of the soil was measured 39° using the shear test (ASTM-D3080), and a bulk density of 1.73 g/cm^3 was calculated. A specific gravity test (G_s) conducted on the soil sample measured a G_s of 2.63 (ASTM-D854). A void ratio derived from these parameters resulted in 0.52. The saturated hydraulic conductivity, k , of the sandy soil had a value of $7.6 \times 10^{-4} \text{ cm/s}$ (Figure 2.).

3.3 Experimental Setup

The model box used for the experiment is shown in Figures 3. and 4. It is 600 mm long, 100 mm wide and 400 mm high. Its walls and partitions are made from transparent plexiglass to visually observe slope model changes and monitor water seepage with a dye and an ultraviolet (UV) LED flashlight.

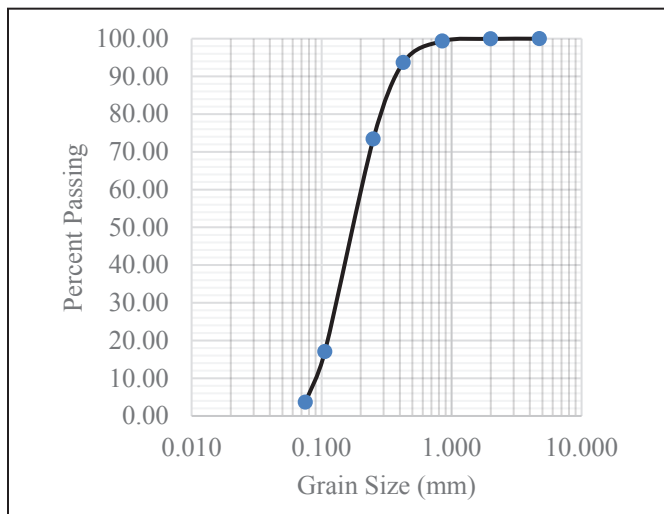


Figure 1. Grain Size Distribution

The box has four compartments: one for the model slope and three sections for the water. The water chamber dimensions on the side views are 100 mm x 400 mm, 100 mm x 400 mm, and 100 mm x 500 mm. The main chamber for the soil slope model has a dimension of 100 mm x 500 mm.

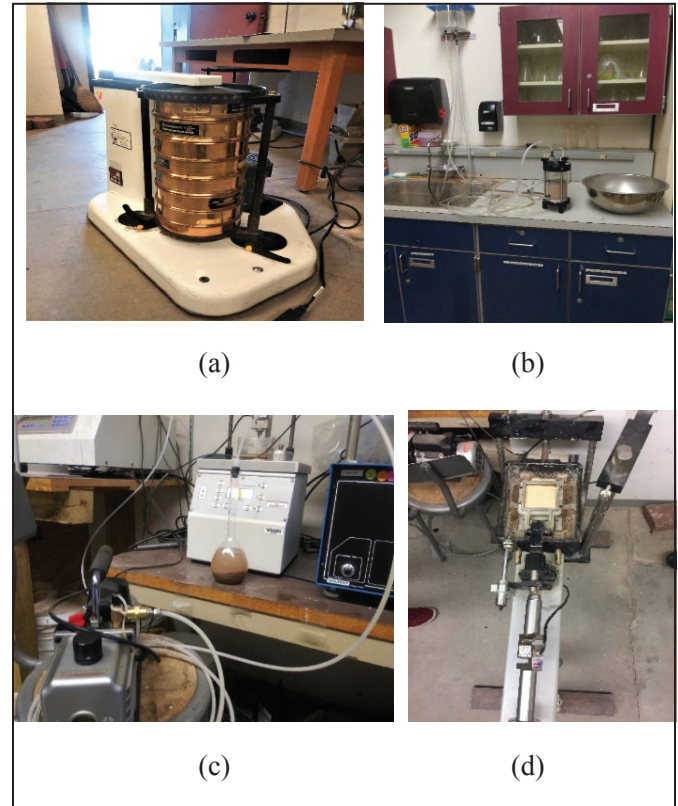


Figure 2. (a) Sieve Analysis test (ASTM D422) (b) Permeability Test (c) Specific Gravity Test (ASTM D-854) (d) Direct Shear Test (ASTM D-3080)

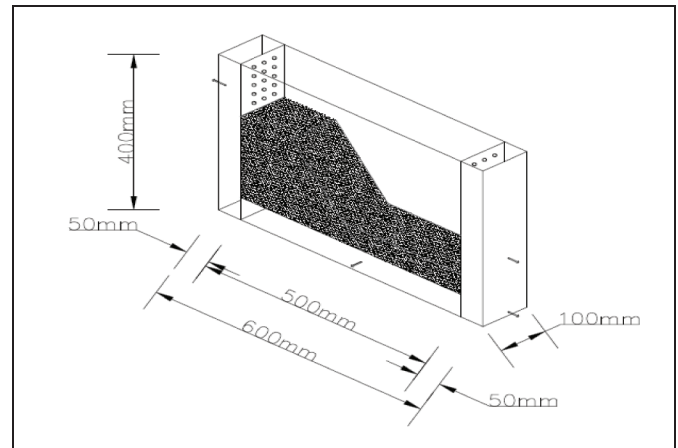


Figure 3. Drawing of the box with dimensions

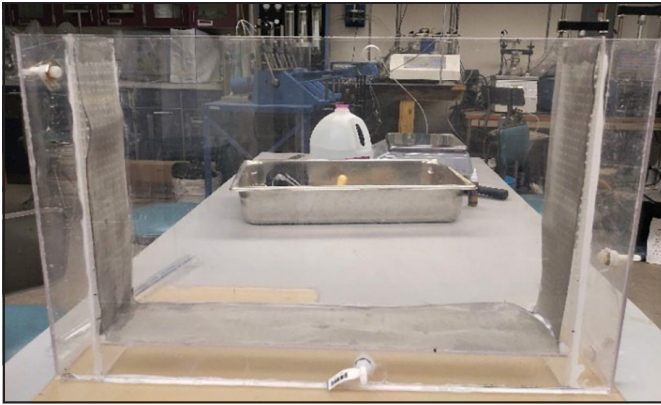


Figure 4. Final image of the box for experiments

Each water chamber plate bordering the slope model has perforations in the plexiglass to allow water to flow in and out of the chamber. The perforations are covered with a fine mesh smaller than the sand particles to prevent any sand particles from entering the water chamber but rather to allow free flow of water through to the soil and prevent flushing of soil particles.

A plain water hose connected to a water container was used to fill in the water chambers. The water container can be elevated or lowered to any level to change the pressure heads. Changes in water level inside the model slope were controlled by injecting water into the sand layer or drawing water out of the sand layer through inlets and outlet points. These helped in the various simulations of constant water rise and drawdown of water.

3.4 Finite Element Modeling

Slope stability programs such as Slide 2D can be used to find safety factors in both soil and rock slopes. The computer program can compute circular and non-circular failure surfaces while evaluating the probability of failure. The software is developed by Rocscience in Canada and can be used for soil and rock slope stability analysis. “Slide2 is simple to use, yet complex models can be created and analyzed quickly and easily. External loading, groundwater, and support can all be modeled in various ways. Individual slip surfaces can be applied to locate the critical slip surface for a given slope. Users can also carry out deterministic (safety factor) or probabilistic (probability of failure) analyses” (Rocscience Slide, 2019).

The two-dimensional finite element method Rocscience was used to analyze various boundary elements. The geometry and soil properties of the model were the same for the soil used for the laboratory experiment. The modeling was used to find the failure planes, pressure heads, flowlines, and flow vectors. Modeling in Slide2 was possible because it can

analyze groundwater, pore-pressure, steady-state, and transient state. In all the analyses, the mesh consisted of 3-node triangular elements and approximately 1500 elements. The default unit weight of 9.81kN/m^3 was used for the density of water and good soil characteristic curve and water content provided to help in the analysis. The numerical results are compared to that of the laboratory test conducted.

3.5 Initial Conditions.

The model slopes were constructed in the middle chamber and compacted in layers of 50 mm. The first layer was spread uniformly and compacted to form the base of the slope. The first experiment was to simulate steady-state flow. The dimensions of the slope were 220 mm high, 100 mm wide, and a crest of 70 mm. The final slope angle was about 35° (Figure 5). After constructing the model slope, the upstream tank was filled gradually with water to the level of 190 mm. The water was kept constant and allowed to flow through the soil and seep to the downstream chamber exit points. To initiate failure, the water level is kept constant until failure occurs. This condition is a resemblance to a steady-state seepage in the real world where water accumulates behind the walls of a slope for a period of time. The condition is mainly seen in tailings dams in the mining industries and natural slopes.

Experiment 2 was to raise the water level gradually until failure occurs. At a slope height of 225 mm, the initial water level was set at 70 mm. The water level is kept constant for 3 minutes and then raised a further 70 mm to 140 mm slope level for another 3 minutes. The last stage was raising and maintaining the water level steady at 215 mm high until failure. The final slope angle for the model was 35° . The image shown in Figure 6. is the setup for the experiment.

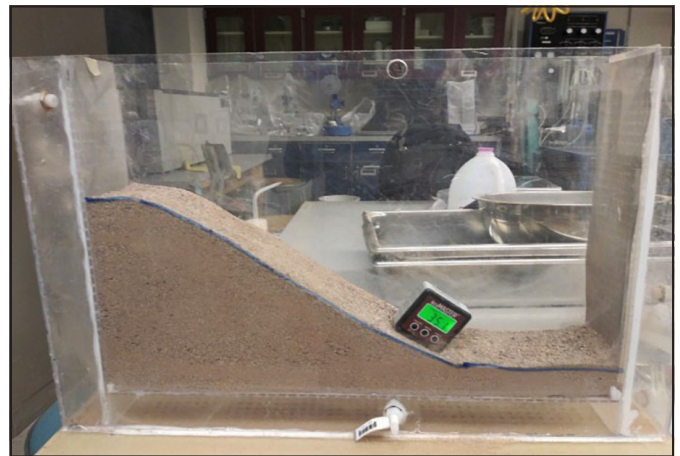


Figure 5. Box of soil sample before experiment 1



Figure 6. Box of soil sample before gradual water rise experiment

The focus for the next test was mainly to study seepage in soil. In this experiment, the bottom chamber was entirely filled with water. A dye was poured in the upslope chamber and water level allowed to rise and flow through the soil slope. A night mode is set and an ultraviolet (UV) flashlight flashed along the water path through the soil (Figure 7). The use of the dye would help tracing the water path as it moves through the soil. Since a night mode is simulated, the UV flashlight was able to detect its path. Finally, a 4K camera is set to film the process for further studies.



Figure 7. Set up for experiment with the camera and dye

3.6 Visual monitoring

A camera was set up to monitor the seepage front using a 4K camera and a dye. The camera recorded the saturation process for seepage and slope movement throughout the experiment. These processes were then compared to the numerical modeling results. The camera was a Sony AX33 4K Handycam (Figure 8). Table 1 shows the technical specifications of the video camera.



Figure 8. The camera for digital video recording

Table 1. Specifications of the video camera

Parameter	Camera
Model	Sony AX33 4K Handycam
Effective pixels (video)	Approximately 8.29 megapixels
Effective pixels (still image)	Approximately 10.3 megapixels
focal length	29.8-298.0 mm
Lens Filter diameter	52 mm

4.0 RESULTS AND DISCUSSION

4.1 Introduction

With laboratory experiments undertaken with pictures of initial conditions and aftermath after failures, the numerical modeling analysis can take place. Numerical models such as Finite Element methods can help simulate slope failures with factor of safety, pressure heads, flow lines, and flow vectors. These experimental works were modeled in the finite element software, and the results were compared to the small-scale slope at the laboratory.

Laboratory experiments for slope failure. The results of the experiments conducted with different scenarios are discussed in this section. In total, four slope stability experiments were conducted with other initial conditions. Experiments 1 and 2 showed similar visual results during the entire time. The first scenario was a steady-state condition with water at the bottom of the chamber (Figure 9), and the second simulated a gradual water rise, which typically represents a tailings dam. The last two (2) focused on the ratio of water level and slope failure (Figure 9).

With water level kept constant at a level of 190 mm of the total slope height of 220 mm, water was allowed to seep through the perforations from the upslope water tank through the soil into the downslope tank. Wetting was seen at the toe of the slope very quickly about 2 minutes from the start of the test. Bulging and pressure ridges at the toe started when the toe was very saturated. This lateral movement was due to pressure build-up from the water seepage. From the 10th minute, tension cracks were spotted close to the toe of the slope, which eventually propagated upslope. The shear stress of the toe diminished, and this made the

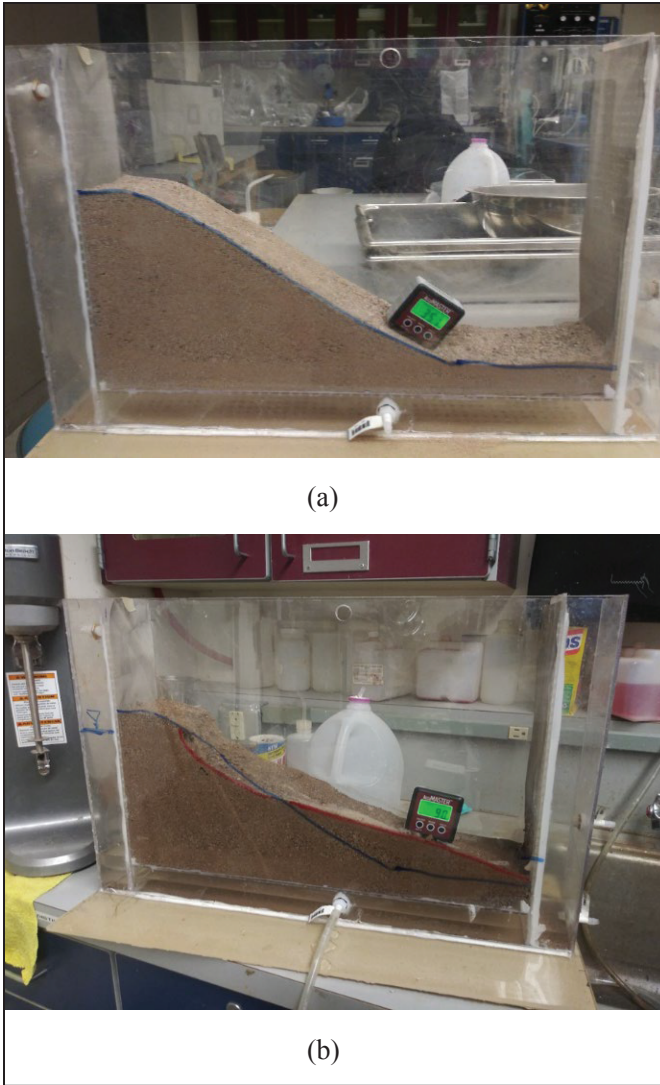


Figure 9. Steady-state failure experiment (a) before and (b) after failure

slope slide. After failure, the slope angle was measured at 9° from the initial 35° . The experiment was terminated after 20 minutes when the failure occurred. The final shape of the slope showed the toe slid, resulting in a collapse to the head of the crest.

The second experiment was a gradual rise in water level to induce slope failure. The water level was kept constant for 3 minutes at each level before rising to the next level. Failure occurred at the last stage when the soil sample was fully saturated.

Experiments 1 and 2 produced similar results, although they had different initial conditions. The results and sequence of events for experiment 2 are tabulated below in Table 2.

A comparison of the slope geometry before and after is shown in Figure 10).

Table 2. Correlation of time, observation, and slope deformation

Time (min)	Upslope Tank water level (mm)	Visual Observation (Saturation zone)	Visual Observation (Deformation)
3	70	Wetting front gradually moving	No deformation of slope
6	140	Wetting at the toe of the slope. Bulging at the toe.	Settlement begins at the crest of the slope
7	140	Lateral movement at toe	Minimum settlement at the crest
9	215	Failure	Slope failure. Settlement measured at 10 mm

The chronology of events for this experiment is similar to that of Jia et al. (2009) where two phenomena were observed, that is settlement of the crest and gradual collapse of the toe induced by wetting.

Firstly, the settlement of the crest of the slope is attributed to the wetting-induced collapse of the saturated area close to the toe. Along with Jia et al. (2009), other research by Tadepalli et al. (1992) also observed a similar wetting-induced collapse where a volumetric strain of 1.1% was measured for the settlement. In this experiment, a 9% settlement was measured. The original slope angle of 35° was reduced to 20° after the failure occurred.

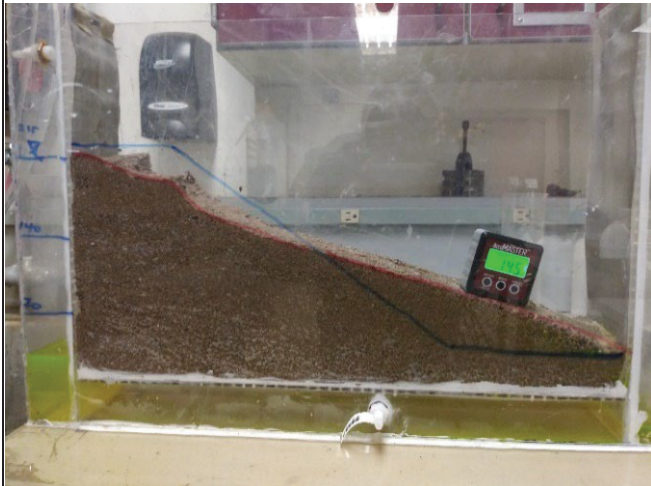
4.3 Finite element modeling for slope failure

During this experiment for slope failure, water was raised at a regular interval. At each level, the water was kept constant for 3 minutes and raised to the next level. At the last level, the slope failed with failure initializing on the slope. The noticeable high hydraulic gradient when water levels rise produces high seepage forces through the soil. These forces cause wetting to be formed early at the toe of the slope. Again, the flow causes pressure ridges at the toe, ultimately resulting in bulging and reduction of shear force at the toe. Failure in the slope occurred primarily due to high hydraulic gradients that resulted in large seepage forces and the decrease of shear strength resulting from high pore pressures.

The factor of safety reduces as the water level rises from an initial of 1.26 to 0.841 at failure. Both Janbu's and Bishop's Methods resulted in a factor of safety less than 1 at failure (Figure 11). This scenario is particularly true to a



(a) Before failure



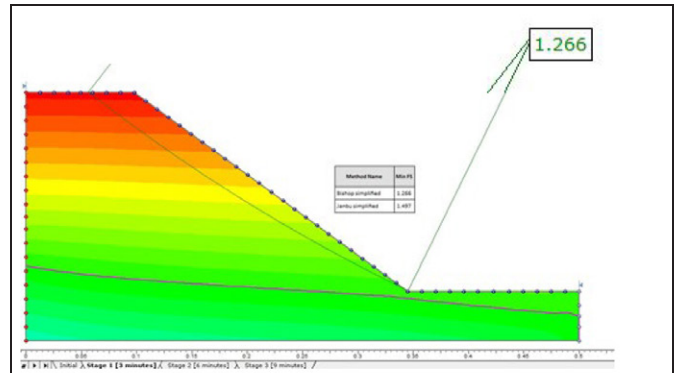
(b) After failure

Figure 10. Experiment of gradual water rise (a) before failure (b) after failure

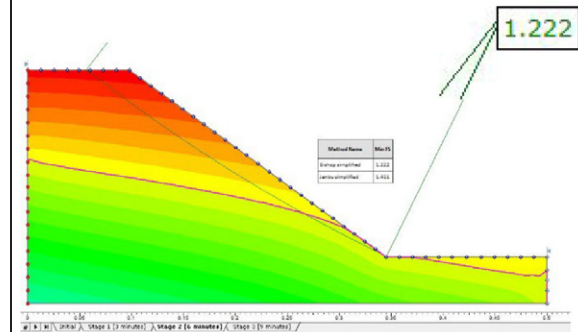
tailings dam when gradual impoundment over time reduces the factor of safety of the embankment

Another experiment was conducted to ascertain the stability of a slope with the presence of groundwater.

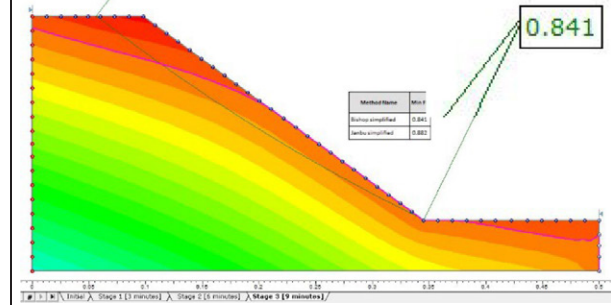
In this experiment, water level was kept constant in the bottom chamber and seepage allowed from the upslope tank downslope. The pressure from the upslope tank into the bottom chamber creates an uplift force downslope which contributes to the instability of the slope. Firstly, the toe becomes very unstable and loose and forces the crest to slide. The flow vectors see such forces in the groundwater model where the uplift force moves from the bottom chamber to the toe. The steady-state analysis showed a factor of safety of 1.32 and 0.715 before and after failure, respectively (Figure 12).



(a) The factor of safety at 3 minutes



(b) The factor of safety at 6 minutes



(c) The factor of safety at the failure at 9 minutes

Figure 11. Factor of safety of slopes with time

It can be concluded from the images that the presence of water and the increase in pore pressure contributes significantly to the stability of the slope.

4.4 Experiment for seepage front (Steady-state and Transient)

Seepage is a complex phenomenon in soil mechanics. A seepage front migrates throughout a slope when the soil particles come into contact with water. Water moves from

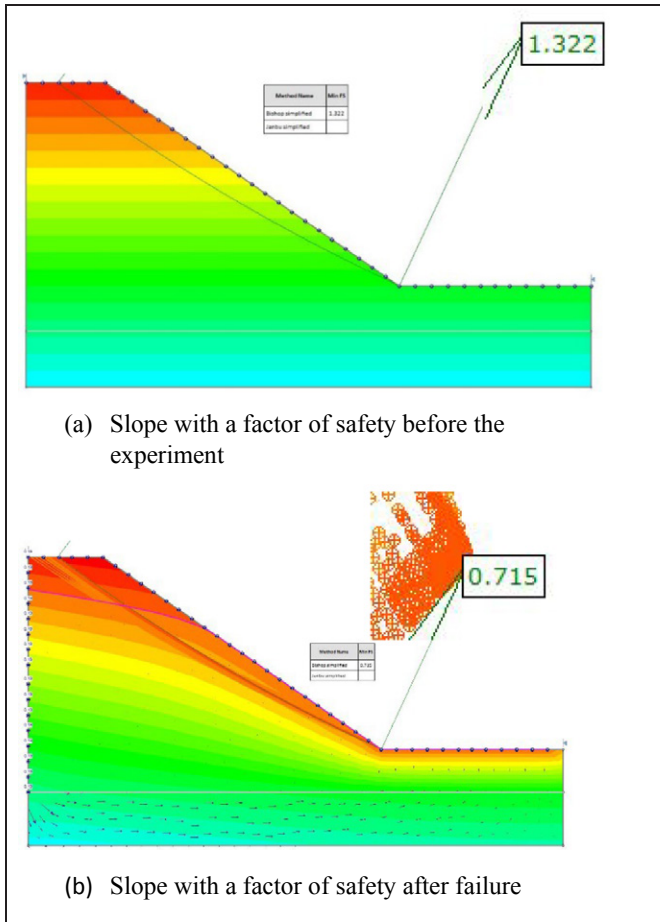


Figure 12. Slope with factor of safety before and after the experiment

an area of higher potential energy to one of lower potential energy and there are many factors that determine this movement. The various energy that exists includes gravitational potential energy and matric potential, which exist in the saturated soil. Soil that has its pores not filled has a matric potential of zero, and the total potential is the sum of the gravitational and the matric.

Seepage front moves in the soil due to the differences in the potential energy. As the water level increases in the left chamber, the pressure increases, driving the forces to move through the soil. Studies of seepage front were conducted on three experiments. The first experiment looked at groundwater increase with a water reservoir beneath the slope (Figure 13). In the test for seepage front where water is kept constant in the bottom chamber, water flows from the left chamber seeping through the bottom water and then finally seen at the toe of the slope. The seepage is seen while the dye moves through the water. The flow vectors and flow lines show the movement and path of water through the soil. It is initially seen moving through the bottom of the soil and through the bottom

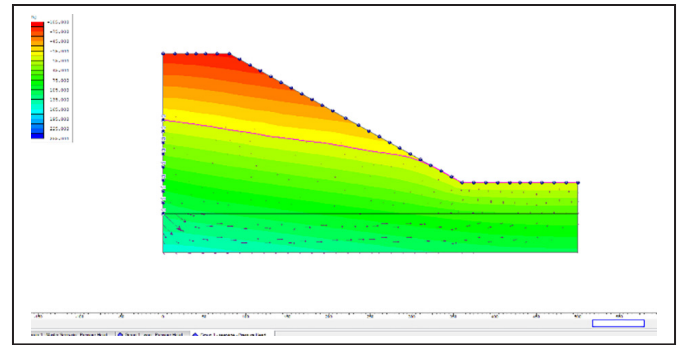


Figure 13. Steady-state seepage

chamber of water and then the curve moves towards the toe. Contours showing pressure differences also indicate high pressures in the soil below the water level. Low pore pressures are also seen above the seepage front in yellow and red color. This is depicted in all the models shown.

The next two experiments looked at seepage without water in the bottom chamber since the base was sealed watertight. In the initial condition, water was allowed to fill the left chamber almost to the level of the slope and kept constant for 5 minutes. The water was then allowed to drawdown and drain through the soil. A transient analysis was then conducted in Rocscience Slide to compare that of the experiment. The analysis showed a gradual seepage front movement. During the last stages, the change was very insignificant hence the difficulty of seeing the difference in the seepage front (Figure 14).

The figure shows the movement of the seepage front with time through the soil sample. The contours show pore pressures with blue being the highest to the least of red color.

4.5 Ratio of water level, slope height, and slope failure

Experiments were conducted to compare the ratios of water level, slope height, and slope failure. During these experiments, three (3) slope heights were chosen; 280 mm, 225 mm, and 150 mm. In all the tests, the slope failed at water levels 270 mm, 215 mm, and 145 mm, respectively. It shows an approximate 96% water level for failure to occur. This is consistent with the experiment by Jia et al. (2009), where the experimental slope failed at a 93.4% water level to slope height ratio. The results are illustrated in the graph below (Figure 15).

Failure occurs at a water level to slope height ratio of 1.04 when the soil is almost fully saturated. Again, at the very high-water level, the gravitational potential energy is also high, which reduces the shear force at the toe of the slope. This causes the toe failure, hence causing the global failure of slope.

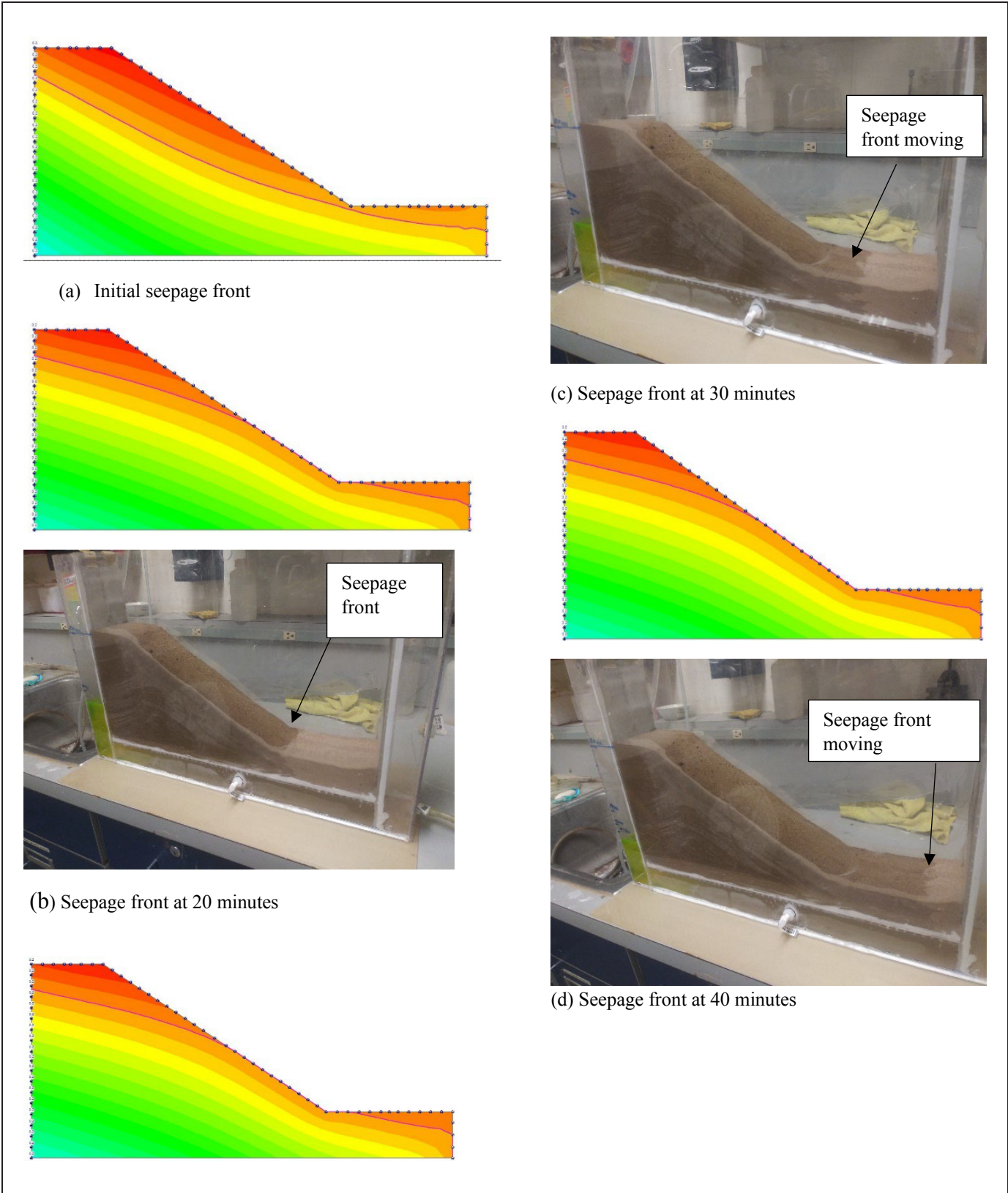


Figure 14. Transient seepages of all stages (continues)

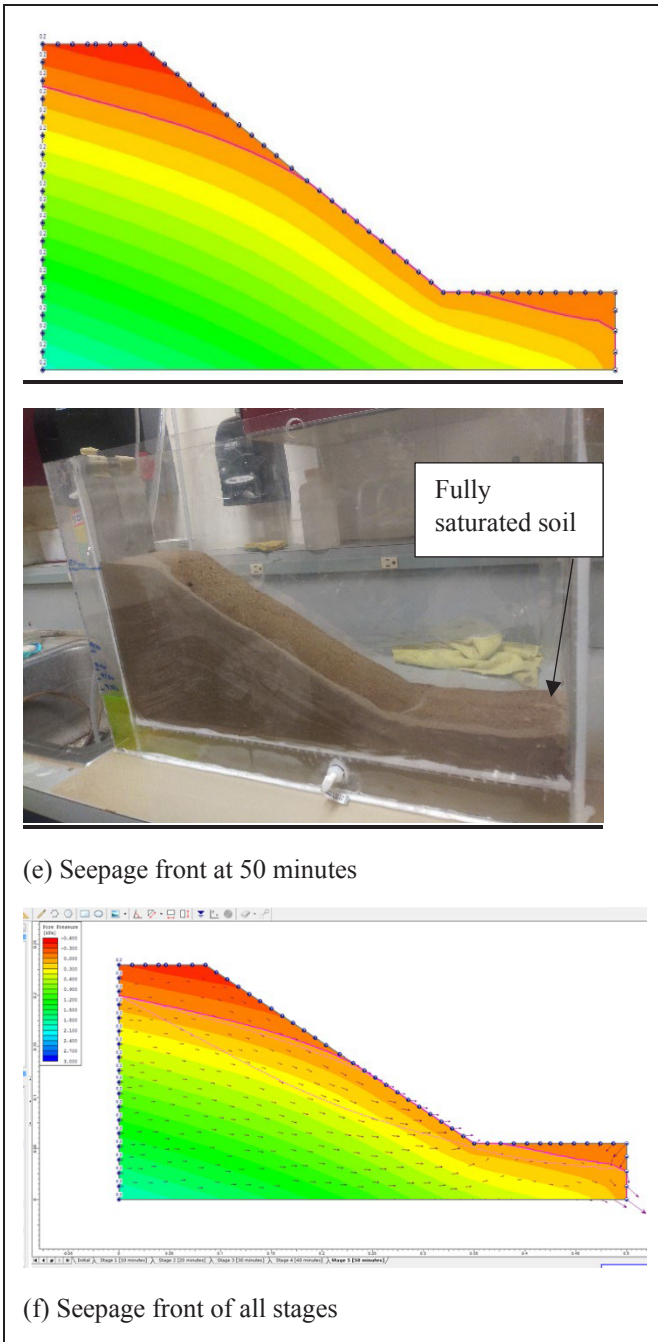


Figure 14. Transient seepages of all stages (continued)

5.0 CONCLUSIONS AND RECOMMENDATIONS

5.1 Introduction

This research studied the seepage of water through soil and slope failures. A test apparatus was designed to contain soil, which allowed for water to seep through to simulate several conditions. This study made use of a dye and UV flashlight

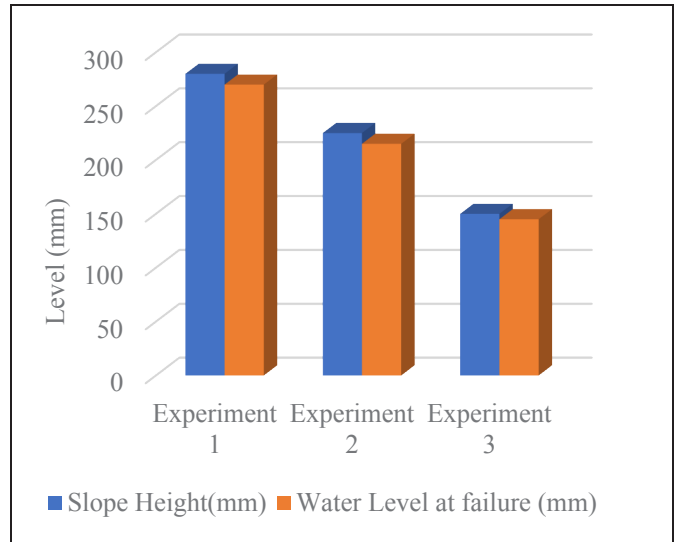


Figure 15. Comparison of slope height to water level at failure

to study the seepage front in soil. Additionally, slope behavior was observed when pore pressure was increased to induce failure. This chapter provides a summary of the results of the study and the conclusion made. Recommendations are then given for further studies.

5.2 Conclusions

Seepage and slope stability are major issues facing the mining industry. Tailings dam failure in recent years has been on the increase, which makes it very important to study the movement of water through soil.

In this study, transparent plexiglass was used to help monitor the seepage front easily and detect slope failure. Other materials, such as wood and glass, were not preferred for several reasons, including the difficulty of joining the material.

The experimentally induced slope failure results were created effectively in models in the Rocscience slide. The models showed results similar to those of the experiments conducted. These models were used to study the seepage front of water through soil and simulate slope failures using conditions similar to those in the lab.

These models were used to find the safety factor for each scenario by comparing it to the slope at failure. It was found that the slope failed when the water level was about 96% of the slope height. These are due to the soil being fully saturated and the shear stress at the toe being almost zero. Further studies should be performed to determine the contribution of soil type and friction angle on these failures.

The study of the seepage front concluded that hydraulic gradient and potential energy determine water flow through

the soil. Water moves from a higher potential energy to a low potential energy in unsaturated soil. When soil gets attracted to water, this attraction is carried on to surrounding grains. From the result of the laboratory experiments, it is apparent that the movement of water depends very much on the permeability of the soil.

5.3 Recommendation for future work

This study has used an ultraviolet-sensitive dye, night mode, and a high-resolution camera to study water movement through the soil. To improve results using this method, it would be beneficial to use a high-resolution video camera again and study seepage by frame-by-frame and seconds analysis. Besides, different soil material layers should be used for slope stability analysis to ascertain the failure of such materials. Moreover, instruments such as piezometers and inclinometers should be used to improve results on slope movement during monitoring.

REFERENCES

- [1] Anderson, S. A., and Thallapally, L. K. (1996), "Hydrologic response of a steep tropical slope on heavy rainfall." Proc., 7th Int. Symposium On Landslides, Balkema, Rotterdam, The Netherlands, Vol. 3, 1489–1495.
- [2] Cai, F. and Ugai, K. (2004). "Numerical analysis of rainfall effects on slope stability." *International Journal of Geomechanics*, 4(2), 69-78.
- [3] Cho, S. E. (2009). "Infiltration analysis to evaluate the surficial stability of two-layered slopes considering rainfall characteristics." *Engineering Geology*, 105, 32-43.
- [4] Chin-Chuan H, Chien-Li L. (2013) simulation of subsurface flows associated with rainfall-induced shallow slope failures
- [5] Eckersley, D. (1990). Instrumented laboratory flow slides. *Geotechnique* 40(3), pp. 489-502
- [6] Fannin, R.J., and Jaakkola, J. (1999). "Hydrological response of hillslope soils above a debris slide headscarp." *Can. Geotech. J.*, 36, 1111–1122.
- [7] Fredlund, D. G., and Rahardjo, H. 1993. *Soil Mechanics of Unsaturated Soils*. New York, N.Y John Wiley and Sons, Inc.
- [8] Gerscovich, D. M. S., Vargas, E. A., and de Campos, T. M. P. (2006). The evaluation of unsaturated flow in a natural slope in Rio de Janeiro, Brazil." *Engineering Geology*, 88, 23-40.
- [9] G.W. Jia, Tony L.T. Zhan, Y.M. Chen, D.G. Fredlund (2009) Performance of a large-scale slope model subjected to rising and lowering water levels
- [10] Johnson, K. A., and Sitar, N. (1990). Hydrologic conditions leading to debris flow initiation. *Can. Geotech. J.*, 27_6_, 789–801.
- [11] Kim, J., Jeong, S., Park, S., and Sharma, J. (2004). "Influence of rainfall-induced wetting on the stability of slopes in weathered soils." *Engineering Geology*, 75, 251-262.
- [12] Martin, T.E. and E.C. McRoberts 1999. Some considerations of the stability analysis of upstream tailings dams. *Proceedings, Tailings and Mine Waste'99*, Fort Collins, Colorado
- [13] Mitchell J.K (2005) Components of pore water pressure and their engineering significance.
- [14] Montrasio, L., Valentino, R., and Losi, G. L. (2009). "Rainfall induced shallow landslides: A model for the triggering mechanism of some case studies in Northern Italy." *Landslides*, 6, 241-251.
- [15] Rahardjo, H. _1999_. "The effect of rainfall on the slope stability of residual soil in Singapore." Report Research Project, Nanyang Technological University, Jurong, Singapore.
- [16] Rahimi, A., Rahardjo, H., and Leong, E. C. (2010). "Effect of hydraulic properties of soil on rainfall-induced slope failure." *Engineering Geology*, 114, 135-143.
- [17] Spence K.J and Guymer I. 1997. Small scale Laboratory flow slides. *Geotechnique* 47:915-932 Totonchi, A., Askari, F. & Farzaneh, O. (2012). 3D stability analysis of concave slopes in plan view using linear finite element and lower bound method. *Iranian Journal of Science and Technology, Transactions of Civil Engineering*, Vol. 36, No. C2, pp. 181-194.
- [18] Tu, X. B., Kwong, A. K. L., Dai, F. C., Tham, L. G., and Min, H. (2009). "Field monitoring of rainfall infiltration in a loess slope and analysis of failure mechanism of rainfall-induced landslides." *Engineering Geology*, 105, 134-150.
- [19] Tadepalli, R., Rahardjo, H., Fredlund, D.G., 1992. Measurements of matric suction and volume changes during inundation of collapsible soils. *Geotechnical Testing Journal, ASTM*, 15 (2), 115–122.
- [20] Chen, Qun and Zhang L.M." Three-dimensional analysis of water infiltration into the Gouhou rockfill dam using saturated–unsaturated seepage theory"

Experimental Study on Position Evolution and Load Transfer Law of Support in Large Dip Angle Stope Based on Digital Twin

Panshi Xie

Yan Chen

Shaogang Wu

Yang Hang

Key Laboratory of Western Mine Mining and Disaster Prevention, Ministry of Education, Xi'an University of Science and Technology, Xi'an, China; School of Energy, Xi'an University of Science and Technology, Xi'an, China

ABSTRACT

In order to realize the intelligent mining of coal seam with large dip Angle, this paper adopts the methods of large proportion variable Angle loading threedimensional physical simulation experiment, numerical simulation and field measurement with digital twin technology. The hydraulic support with large dip Angle and large mining height is used as the prototype to design the physical entity model of 1:5 hydraulic support, combined with modeling and graphics rendering technology. Angle, displacement and load sensors were selected and placed to realize the data channel between the lower machine and the upper computer of the digital twin system, so that the position and load data of the physical entity model and the twin model of the laboratory hydraulic support could be shared in real time. Moreover, the multi-dimensional dynamic and static load transfer law and the position evolution characteristics of the support and surrounding rock under different inclination angles were analyzed. The results show that: with the

increase of the Angle of the working face, first, the initial support force required by the support decreases, and the damage degree of the roof increases; When the roof is soft, the lifting operation can avoid the instability of the support to a certain extent. Second, under the action of positive pressure, the load of the top beam under different angles is balanced; Under the backpushing action, the load in the upper inclined area of the shield beam increases gradually, while the load in the lower inclined area decreases gradually. Under the lateral push, the load changes periodically, and the load in each cycle is increased compared with that in the previous cycle. Third, the numerical simulation analysis shows that the load on the lower bracket is less than that on the upper bracket, and the load on the bottom of all the columns is greater than that on the middle and upper brackets. In order to reduce the impact of the columns on the bottom plate or the base, it is necessary to improve the anti-subsidence ability of the base. Finally, according to the research results, the improvement and optimization measures of the support are put forward, and the field test shows that these measures effectively solve the problems of sinking, sliding and tipping of the support in the working face with large inclination Angle, and obtain good application results.

Supported by the National Natural Science Foundation of China (Grant No.52174126 and 52104147), Shaanxi Outstanding Youth Science Foundation Project (2023-JC-JQ-42), Shaanxi University Youth Innovation Team Project